nature immunology

The favorable *IFNL3* genotype escapes mRNA decay mediated by AU-rich elements and hepatitis C virus–induced microRNAs

Adelle P McFarland[1], Stacy M Horner[1,7], Abigail Jarret[1], Rochelle C Joslyn[1], Eckart Bindewald[2], Bruce A Shapiro[3], Don A Delker[4], Curt H Hagedorn[4,7], Mary Carrington[5,6], Michael Gale Jr[1] & Ram Savan[1]

IFNL3, **which encodes interferon-λ3 (IFN-λ3), has received considerable attention in the hepatitis C virus (HCV) field, as many independent genome-wide association studies have identified a strong association between polymorphisms near *IFNL3* and clearance of HCV. However, the mechanism underlying this association has remained elusive. In this study, we report the identification of a functional polymorphism (rs4803217) in the 3′ untranslated region (UTR) of *IFNL3* mRNA that dictated transcript stability. We found that this polymorphism influenced AU-rich element (ARE)-mediated decay (AMD) of *IFNL3* mRNA, as well as the binding of HCV-induced microRNAs during infection. Together these pathways mediated robust repression of the unfavorable *IFNL3* polymorphism. Our data reveal a previously unknown mechanism by which HCV attenuates the antiviral response and indicate new potential therapeutic targets for HCV treatment.**

Hepatitis C virus (HCV) infects over 150 million people worldwide. Treatment for chronic infection with HCV is based on interferon therapy in combination with ribavirin. A newly approved triple-combination treatment, which includes direct-acting antiviral agents, has improved cure rates to greater than 60% (ref. 1). However, emergence of therapy-resistant HCV variants in patients treated with direct-acting antiviral agents has become an important concern[1,2]. Genome-wide association studies have identified three single-nucleotide polymorphisms (SNPs) near *IFNL3* (which encodes interferon-λ3 (IFN-λ3), also known as interleukin 28B (IL-28B)) strongly associated with response of HCV-infected patients to therapy[3–6] and natural clearance of infection with HCV[6,7]. However, the functional polymorphism that mediates those associations has remained unknown.

IFN-λ3 is a member of the IFN-λ cytokine family, which is composed of IFN-λ1 (IL-29), IFN-λ2 (IL-28A) and IFN-λ3 (IL-28B), all of which are encoded by genes clustered on human chromosome 19 (refs. 8,9). The expression of members of the IFN-λ family is induced in both hematopoietic and nonhematopoietic cells by various viruses that infect humans[10]. Unlike IFN-α/β signaling, IFN-λ signaling exhibits cellular specificity, as the receptor for IFN-λ is narrowly distributed on epithelial cells, melanocytes and hepatocytes, which suggests that the IFN-λ family of cytokines evolved to specifically protect the epithelium from viral invasion[11]. These are potent antiviral cytokines able to inhibit HCV replication and, when paired with direct-acting antiviral agents, have shown antiviral activity against HCV comparable to that of IFN-α[12,13]. IFN-λ and IFN-α induce a similar repertoire of interferon-stimulated genes (ISGs) in human hepatocytes, although treatment with IFN-λ induces a steady increase in expression instead of the rapid peak and decrease seen with IFN-α[12,14]. Several confounding studies have shown that the unfavorable *IFNL3* genotype is associated with higher pre-therapy expression of ISGs during HCV infection[15,16]. However, correlations between ISG expression and *IFNL3* genotype have been shown to differ by cell type[16], and when treatment response (those who do not respond versus those who do respond) is stratified by *IFNL3* genotype, there is no difference in total mean baseline ISG expression[17]. This suggests that *IFNL3* genotype and pre-therapy expression of ISGs are independent predictors of interferon responsiveness in patients with chronic HCV infection[17].

While five studies have found a correlation between *IFNL3* genotype and expression of *IFNL3* and/or IFN-λ3[3,4,18–20], whereby higher expression of *IFNL3* and/or IFN-λ3 is associated with clearance of HCV, three studies have found no such association[5,15,21]. One study demonstrating an association in normal liver has also found that people with the favorable *IFNL3* genotype have the highest expression

[1]Department of Immunology, University of Washington, Seattle, Washington, USA. [2]Basic Science Program, Leidos Biomedical Research, Frederick National Laboratory for Cancer Research, Frederick, Maryland, USA. [3]Center for Cancer Research Nanobiology Program, National Cancer Institute, Frederick, Maryland, USA. [4]Divison of Gastroenterology, Hepatology and Nutrition, School of Medicine, University of Utah, Salt Lake City, Utah, USA. [5]Cancer and Inflammation Program, Laboratory of Experimental Immunology, Science Applications International Corporation–Frederick, Frederick National Laboratory for Cancer Research, Frederick, Maryland, USA. [6]Ragon Institute of Massachusetts General Hospital, Massachusetts Institute of Technology and Harvard University, Boston, Massachusetts, USA. [7]Present addresses: Department of Molecular Genetics and Microbiology, Center for Virology, Duke University Medical Center, Durham, North Carolina, USA (S.M.H.), and Department of Internal Medicine, University of Arkansas for Medical Sciences, Little Rock, Arkansas, USA (C.H.H.). Correspondence should be addressed to R.S. (savanram@uw.edu).

Received 21 August; accepted 24 September; published online 17 November 2013; doi:10.1038/ni.2758

of ISGs[19]. As noted above, that is opposite to what has been found by baseline gene expression analyses of patients with chronic HCV infection, which suggests that chronic infection dysregulates the immune response and makes correlations between *IFNL3* genotype and gene expression less straightforward. Furthermore, cytokine-encoding mRNAs are extremely labile in nature, which makes them very difficult to measure in biological samples. As there are substantial data supporting a correlation between *IFNL3* genotype and expression of *IFNL3* and/or IFN-λ3, we sought to determine whether there is a functional variant that mediates differences in the expression of this cytokine.

Four candidate causal SNPs have been identified that are in linkage disequilibrium with the SNPs identified by genome-wide association studies[22–24]. None of those candidate SNPs, which are located in the *IFNL3* promoter, intron, coding region or 3′ untranslated region (UTR), have been previously shown to functionally affect *IFNL3* expression. As the expression of cytokine-encoding genes is under tight post-transcriptional control[25], we hypothesized that variation in the 3′ UTR of *IFNL3* (SNP rs4803217) might alter mRNA turnover and protein expression by interfering with regulatory elements. The rs4803217 variant with the unfavorable thymidine (T) residue rather than guanosine (G) at position 53 in the 3′ UTR is most common among African populations (T = 55%; G = 45%) and least common in Asians (T = 7%; G = 93%; http://browser.1000genomes.org/Homo_sapiens/Variation/Population?db=core;r=19:39733720-39734720;v=rs4803217;vdb=variation;vf=3692579). A similar frequency is seen for the 'tag' (i.e., marking and nonfunctional) SNP rs12979860 (identified by genome-wide association studies), which is in linkage disequilibrium with the SNP in the 3′ UTR. The high frequency of the unfavorable T polymorphism in African populations has been proposed as the reason for the finding that African patients are less likely to clear HCV than are Asian patients[7]. In this study, we found that the *IFNL3* SNP rs4803217 was responsible for robust expression differences between the genotype (G/G) associated with clearance of HCV (the 'clearance genotype') and the genotype (T/T) associated with no clearance of HCV (the 'nonclearance genotype') and thus identified rs4803217 as a critical functional SNP that directed the outcome of HCV infection by controlling the stability of *IFNL3* mRNA. Our data revealed that HCV was able to induce two microRNAs (miRNAs), miR-208b and miR-499a-5p, that target the polymorphic region of the *IFNL3* 3′ UTR. This is a previously unknown strategy by which HCV evades the immune system and suggests these miRNAs could be therapeutic targets for restoring the host antiviral response.

RESULTS

Influence of SNP rs4803217 in the 3′ UTR of *IFNL3* mRNA

We evaluated the influence of the 3′ UTR SNP rs4803217 on the post-transcriptional regulation and stability of *IFNL3* mRNA. We generated full-length 3′ UTRs of *IFNL3* with either T (*IFNL3*-T) or G (*IFNL3*-G) at position 53 in the 3′ UTR and cloned those downstream of the gene encoding firefly luciferase, for use as a reporter (**Fig. 1a** and **Supplementary Fig. 1a**,**b**), then transfected human hepatoma (HepG2 and Huh7) cells with those constructs and measured luciferase activity. The *IFNL3*-T 3′ UTR conferred 30–40% lower luciferase activity than did the *IFNL3*-G 3′ UTR (**Fig. 1b**). We next assessed the effect of rs4803217 on mRNA stability. Analysis of the firefly luciferase–encoding mRNA that remained in HepG2 cells after treatment with actinomycin D revealed that mRNA bearing the *IFNL3*-T 3′ UTR decayed twice as fast as that bearing the *IFNL3*-G 3′ UTR (**Fig. 1c**), which demonstrated that this single nucleotide change affected the general stability of the mRNA transcript. Together these data demonstrated a strong influence of rs4803217 on the stability and expression of *IFNL3*.

As with many cytokine-encoding genes, the 3′ UTR of *IFNL3* contains *cis*-acting stretches of adenosine-uridine repetitions (AU-rich elements (AREs)), at positions 33–37, 58–62 and 79-83 (**Fig. 1d** and **Supplementary Fig. 1a**). AREs are perhaps the best-known determinants of mRNA stability, as degradative RNA-binding proteins can bind to AREs, which leads to ARE-mediated decay (AMD) of the transcript[26]. *IFNL3* can be categorized as a class I ARE-containing mRNA, as it has three copies of the pentameric motif AUUUA. We generated luciferase reporter constructs containing 3′ UTRs of *IFNL3* mRNA with disrupted ARE motifs (ΔARE), in which the original sequence of AUUUA was mutated to AUCUA (**Fig. 1d**), and measured luciferase expression in HepG2 cells transfected with those constructs. Both the *IFNL3*-T(ΔARE) 3′ UTR and the *IFNL3*-G(ΔARE) 3′ UTR were completely protected from repression and demonstrated equivalent 'rescue' relative to that of the *IFNL3*-T and *IFNL3*-G 3′ UTRs (**Fig. 1e**). These data demonstrated that the AREs in the *IFNL3* 3′ UTR were functional and facilitated AMD of this transcript.

The difference between *IFNL3*-T expression and *IFNL3*-G expression was not maintained in the absence of AMD (**Fig. 1e**), which suggested that AMD may have had a greater effect on the stability of *IFNL3*-T. To explore this further, we generated luciferase reporter constructs with individual ARE sites (1–3) disrupted in the *IFNL3*-T 3′ UTR or *IFNL3*-G 3′ UTR. We observed that the difference in the regulation of *IFNL3*-T and *IFNL3*-G was maintained only in the presence of both ARE 1 and ARE 2 and did not require activity at ARE 3 (**Fig. 1f**). However, when we disrupted ARE 1 or ARE 2 individually, the difference in the degradation of the *IFNL3*-T 3′ UTR and that of the *IFNL3*-G 3′ UTR was not significant (**Fig. 1f**). This suggested that ARE 3 participated in equal degradation of both variants, whereas the combined activity of ARE 1 and ARE 2 facilitated different degrees of AMD. It is possible that the location of rs4803217 between ARE 1 and ARE 2 alters the local secondary structure of the mRNA and thereby disrupted the ability of ARE-binding proteins to effectively degrade the *IFNL3*-T mRNA. Comparison of predicted base-pair probabilities of the *IFNL3*-T 3′ UTR versus that of the *IFNL3*-G 3′ UTR showed that the only sites with significant differences were ARE 1, ARE 2 and the SNP rs4803217 (**Supplementary Fig. 1c**). Structural changes in motif-defining sequences, such as AREs, in the 3′ UTR can have functional consequences by influencing accessibility to *trans*-acting RNA-decay factors[27].

The cytokines IFN-λ2 and IFN-λ3 have 98% amino acid sequence similarity[8,9] and 95% sequence identity in the 3′ UTRs of their mRNA (**Supplementary Fig. 1a**). In contrast, the 3′ UTRs of *IFNL3* and *IFNL1* have a low sequence identity (47%) but do share conservation in the AREs (**Supplementary Fig. 2a**). The T variant of rs4803217 in the 3′ UTR of *IFNL3* is the ancestral allele, and only in humans has a G variant emerged (**Supplementary Fig. 2b**). Notably, there are no known variants of *IFNL2* (which encodes IFN-λ2) associated with clearance of HCV. In contrast to type I and type II interferons, members of the IFN-λ family have been strongly affected by positive selection[28]. That analysis revealed that five SNPs near or in *IFNL3*, including rs4803217, have rapidly increased in frequency. However, position 53 (which aligns with rs4803217 in the 3′ UTR of *IFNL3*) is 'fixed' with a T nucleotide in the 3′ UTR of *IFNL2*. To understand why the polymorphism at this site was evolutionary selected for in *IFNL3* but not *IFNL2*, we cloned into luciferase reporter constructs the full-length *IFNL2* 3′ UTR as well as one in which the native T nucleotide at position 53 was replaced with G (**Supplementary Fig. 2c**). When expressed in HepG2 cells, the luciferase activity of the construct with wild-type *IFNL2* 3′ UTR (T at position 53) was significantly higher (+15%) than that of the construct with *IFNL3*-T (**Fig. 1g**). The luciferase

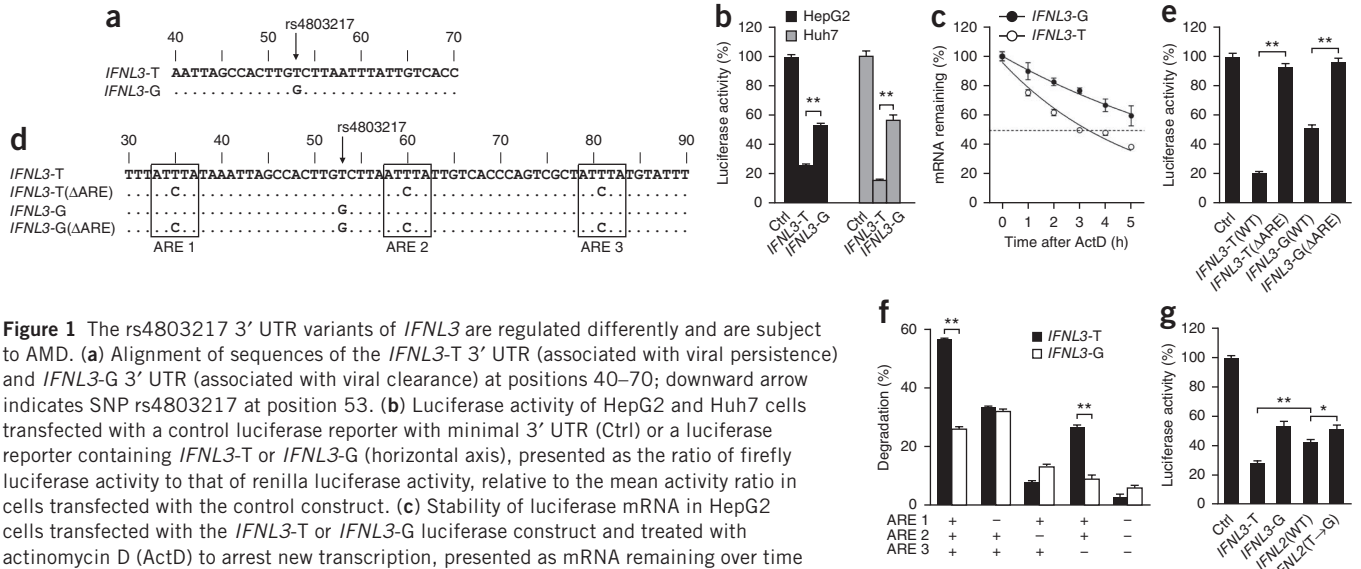

Figure 1 The rs4803217 3′ UTR variants of *IFNL3* are regulated differently and are subject to AMD. (**a**) Alignment of sequences of the *IFNL3*-T 3′ UTR (associated with viral persistence) and *IFNL3*-G 3′ UTR (associated with viral clearance) at positions 40–70; downward arrow indicates SNP rs4803217 at position 53. (**b**) Luciferase activity of HepG2 and Huh7 cells transfected with a control luciferase reporter with minimal 3′ UTR (Ctrl) or a luciferase reporter containing *IFNL3*-T or *IFNL3*-G (horizontal axis), presented as the ratio of firefly luciferase activity to that of renilla luciferase activity, relative to the mean activity ratio in cells transfected with the control construct. (**c**) Stability of luciferase mRNA in HepG2 cells transfected with the *IFNL3*-T or *IFNL3*-G luciferase construct and treated with actinomycin D (ActD) to arrest new transcription, presented as mRNA remaining over time relative to that at 0 h, set as 100%. Half-lives (50% mRNA remaining (dashed line)): *IFNL3*-G 3′ UTR, 7.0 h ($R^2 = 0.82$); *IFNL3*-T 3′ UTR, 3.3 h ($R^2 = 0.95$). (**d**) Alignment of *IFNL3* 3′ UTR sequences (positions 30–90) showing ARE 1–ARE 3 (boxed) and mutations (ATTTA→ATCTA) introduced to disrupt the motifs (ΔARE). (**e**) Luciferase activity of HepG2 cells transfected with a control luciferase reporter or a luciferase reporter containing wild-type *IFNL3*-T (*IFNL3*-T(WT)), *IFNL3*-T(ΔARE), wild-type *IFNL3*-G (*IFNL3*-G(WT)) or *IFNL3*-G(ΔARE), presented as in **b**. (**f**) Degradation of luciferase reporters containing *IFNL3*-T or *IFNL3*-G with intact (+) or disrupted (–) ARE 1–ARE 3 (below graph), relative to that of the control construct, set as 0%. (**g**) Luciferase activity of HepG2 cells transfected with a control luciferase reporter or a luciferase reporter containing *IFNL3*-T, *IFNL3*-G, wild-type *IFNL2* (*IFNL2*(WT)) or *IFNL2* with substitution of G for T at position 53 of the 3′ UTR (*IFNL2*(T→G)), presented as in **b**. $^*P < 0.05$ and $^{**}P \leq 0.0005$ (two-tailed unpaired *t*-test (**e**,**g**) or two-tailed two-way analysis of variance (**f**)). Data are from one experiment representative of three or more experiments with six replicates per group (**b**,**e**–**g**; mean and s.e.m.) or are from one of three experiments with similar results (**c**; mean ± s.e.m.).

activity of the construct with the *IFNL2* 3′ UTR with substitution of G for T at position 53 was only slightly greater than that of the construct with the wild-type *IFNL2* 3′ UTR (**Fig. 1g**). We also investigated whether an *IFNL2*(ΔARE) 3′ UTR would 'rescue' expression of the luciferase reporter and found that, like the *IFNL3*(ΔARE) 3′ UTRs, it was completely protected from repression (**Supplementary Fig. 2d**). Overall these data indicated that, like *IFNL3* mRNA, *IFNL2* mRNA was subjected to post-transcriptional regulation by AMD but was not degraded to the same extent as was *IFNL3*-T.

Regulation of *IFNL2* and *IFNL3* by miRNAs

As a 3′ UTR variant of *HLA-C* is known to be strongly associated with control of infection with human immunodeficiency virus and to drive high expression of *HLA-C* by escaping regulation by the miRNA miR-148 (ref. 29), we reasoned such a mechanism could act on *IFNL3*. miRNAs are a class of small (~22-nucleotide) regulatory RNA molecules whose main function is to decrease the abundance of protein-encoding mRNA by directly pairing with the 3′ UTR of the target mRNA[30]. Published work has demonstrated that miRNAs can act together with ARE-binding proteins to destabilize cytokine-encoding mRNAs[31]. We investigated whether the 3′ UTR SNP rs4803217, in addition to mediating differences in AMD, could influence recruitment of miRNAs to the 3′ UTR of *IFNL3*. We examined the 3′ UTR sequence around the site of rs4803217 for predicted miRNA-binding sites and identified potential binding sites for hsa-miR-208b and hsa-miR-499a-5p, two miRNAs with identical seed regions in the *IFNL3*-T 3′ UTR and *IFNL2* 3′ UTR (**Fig. 2a** and **Supplementary Fig. 1a**). The SNP rs4803217 with the T-to-G substitution is in the miRNA seed region and would therefore be predicted to prevent the binding of those miRNAs to the *IFNL3*-G 3′ UTR.

MIR208B (hsa-miR-208b) and *MIR499A* (hsa-miR-499) are in the introns of *MYH7* (which encodes myosin heavy chain 7) and *MYH7B* (which encodes myosin heavy chain 7B), respectively (**Fig. 2b**). They are part of a group of miRNAs called 'myomiRs' because of their location and coexpression with their corresponding myosin-encoding genes[32]. A key feature of those myomiRs is their restricted expression to cardiac and slow skeletal muscle, as *MYH7* and *MYH7B* encode the major contractile proteins of muscle. In this context, miR-208b and miR-499a-5p control myosin expression and skeletal myofiber phenotypes by targeting transcriptional repressors of myofiber-encoding genes[32]. As those miRNAs are not normally expressed in the liver and we did not detect their constitutive expression in HepG2 or Huh7 cells, we assessed whether infection with HCV could induce their expression. We found that infection with HCV resulted in the induction of *MYH7* and *MYH7B* and their associated myomiRs (**Fig. 2c**,**d** and **Supplementary Fig. 3a**). Another member of the myomiR family encoded in the myosin-encoding gene *MYH6*, miR-208a, has a seed sequence identical to that of miR-208b and miR-499a-5p and was predicted to target the *IFNL3*-T 3′ UTR, but we did not detect its induction during HCV infection (data not shown). Therefore, in this study, we set out to characterize the effects of the HCV-inducible myomiRs miR-208b and miR-499a-5p on the 3′ UTRs of *IFNL2* and *IFNL3*.

We cotransfected HepG2 cells with miR-208b, miR-499a-5p or negative control mimics and with luciferase reporter constructs containing the *IFNL3*-T, *IFNL3*-G or *IFNL2* 3′ UTR. Both miR-208b and miR-499a-5p significantly reduced the luciferase activity of the *IFNL3*-T 3′ UTR but not the *IFNL3*-G 3′ UTR, relative to that of cells transfected with the negative control mimics (**Fig. 2e**). To determine whether ARE-binding proteins are involved in recruitment of the miRNA-induced silencing complex (miRISC) to the *IFNL3* 3′ UTR, we cotransfected cells with mimics of the myomiRs and the *IFNL3*(ΔARE) luciferase reporter constructs. Similar to results obtained with the *IFNL3*-T and *IFNL3*-G 3′ UTRs, the myomiRs were able to repress the *IFNL3*-T(ΔARE) 3′ UTR but had no significant effect on the

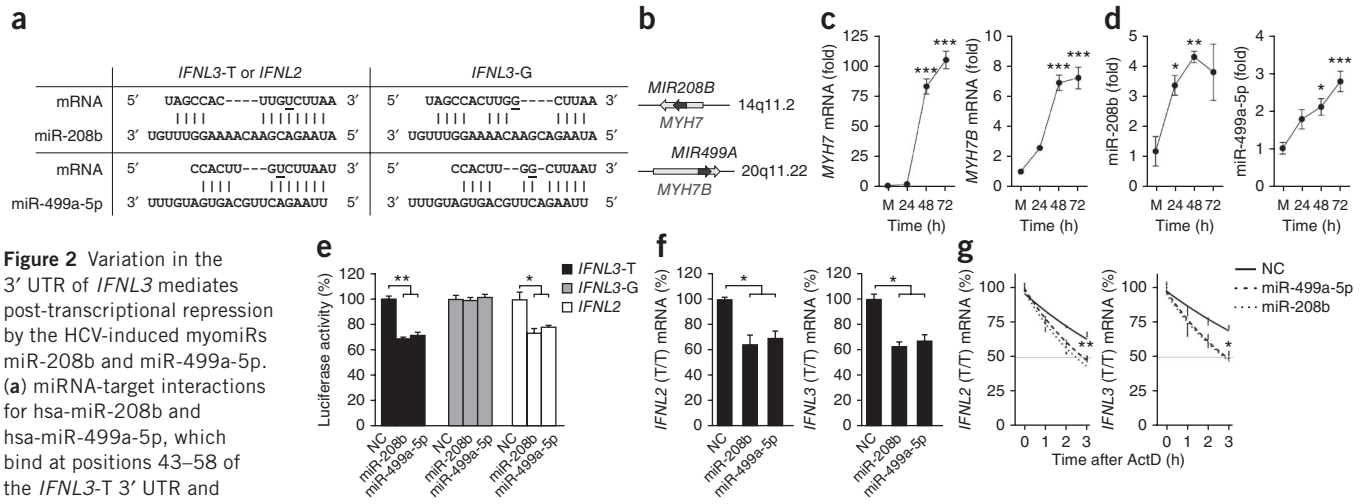

Figure 2 Variation in the 3′ UTR of *IFNL3* mediates post-transcriptional repression by the HCV-induced myomiRs miR-208b and miR-499a-5p. (**a**) miRNA-target interactions for hsa-miR-208b and hsa-miR-499a-5p, which bind at positions 43–58 of the *IFNL3*-T 3′ UTR and *IFNL2* 3′ UTR; the T-to-G substitution in SNP rs4803217 (underlined) is at position 53. (**b**) Chromosomal location of human *MYH7* and *MYH7B* (gray arrows) and their intronic miRNAs *MIR208B* and *MIR499A* (black arrows). (**c**,**d**) Expression of *MYH7* and *MYH7B* mRNA (**c**) and miR-208b and miR-499a-5p (**d**) in Huh7 cells mock infected for 48 h (M) or infected for 24, 48 and 72 h with HCV; results are presented relative to those of mock-infected cells. $^{*}P < 0.05$, $^{**}P < 0.01$ and $^{***}P < 0.001$, compared with mock infection (one-way analysis of variance). (**e**) Luciferase activity in HepG2 cells transfected with luciferase reporter constructs containing the *IFNL3*-T, *IFNL3*-G or *IFNL2* 3′ UTR (key) along with a negative control mimic (NC) or a mimic of miR-208b or miR-499a-5p (horizontal axis), presented as the ratio of firefly luciferase activity to that of renilla luciferase activity, relative to the mean activity ratio of cells transfected with each construct plus the negative control mimic. $^{*}P < 0.01$ and $^{**}P < 0.001$ (unpaired two-tailed *t*-test). (**f**) Expression of *IFNL2* and *IFNL3* mRNA in HepG2 cells transfected with mimics (as in **e**) and then stimulated with poly(I:C), presented relative to that of cells transfected with the negative control mimic, set as 100%. $^{*}P < 0.01$ (unpaired two-tailed *t*-test). (**g**) Stability of *IFNL2* (T/T) and *IFNL3* (T/T) mRNA in HepG2 cells transfected with the HCV PAMP plus mimics (as in **e**), followed by the addition of actinomycin D 16 h after transfection; $R^2 \geq 0.85$ for all curve fits. mRNA half-lives: *IFNL2*, 4.5 h (NC), 2.4 h (miR-208b) and 2.7 h (miR-499a-5p); *IFNL3* mRNA, 5.4 h (NC), 3.1 h (miR-208b) and 3.2 h (miR-499a-5p). $^{*}P = 0.0005$ and $^{**}P < 0.0001$ (F test). Data are pooled from four independent experiments (**c**,**d**; mean ± s.e.m.) or three independent experiments (**f**; mean and s.e.m.), are from one experiment representative of three experiments with six replicates per group (**e**; mean and s.e.m.) or are from one experiment of two experiments with similar results (**g**; mean ± s.e.m.).

IFNL3-G(ΔARE) 3′ UTR (**Supplementary Fig. 3b**). Therefore, ARE-binding proteins were not physically required for recruitment of the miRISC to the *IFNL3*-T 3′ UTR. The luciferase activity of the *IFNL2* 3′ UTR was also significantly reduced by the mimics of the myomiRs but was more resilient against low concentrations of the mimics than was the luciferase activity of the *IFNL3* 3′ UTR (**Fig. 2e** and **Supplementary Fig. 3c**). Overall these results demonstrated that miR-208b and miR-499a-5p directly targeted and mediated degradation of the *IFNL3*-T 3′ UTR and that the SNP rs4803217 with the T-to-G substitution conferred protection against repression by the myomiRs.

We found that the *IFNL3* genotype of our HepG2 cell line is T/T at the site of rs4803217, so we used these cells to study possible regulation of endogenous *IFNL2* and *IFNL3* transcripts by myomiRs. We treated HepG2 cells with the synthetic RNA duplex poly(I:C), which is a ligand of Toll-like receptor 3, and observed peak *IFNL* mRNA expression around 12 h after stimulation (**Supplementary Fig. 3d**). In HepG2 cells transfected with miR-208b, miR-499a-5p or negative control mimics and then stimulated with poly(I:C), both myomiRs significantly repressed expression of *IFNL2* mRNA and *IFNL3* mRNA (**Fig. 2f**). To assess whether that repression was a result of destabilization of the mRNA, we analyzed the stability of the mRNA in the presence of the mimics of the myomiRs after treatment with actinomycin D. To induce expression of *IFNL2* and *IFNL3*, we stimulated HepG2 cells with the HCV 3′ poly-U/UC tract, a pathogen-associated molecular pattern (PAMP) in the 3′ UTR of HCV that has potent immunostimulatory effects on hepatocytes, such as inducing type I interferons[33]. We found strong induction of the expression of both *IFNL2* and *IFNL3* in HepG2 cells by the HCV PAMP (**Supplementary Fig. 3e**). We transfected miR-208b, miR-499a-5p or negative control mimics, as well as the HCV PAMP, into HepG2 cells and arrested new transcription with actinomycin D 16 h after stimulation. We observed that miR-208b and miR-499a-5p each reduced the half-life of *IFNL2* and *IFNL3* mRNA to nearly half that of cells transfected with negative control mimics (**Fig. 2g**).

To support the proposal that these miRNAs directly target endogenous *IFNL2* and *IFNL3* transcripts, we measured the association of *IFNL2* and *IFNL3* mRNA with the miRISC. We transfected HepG2 cells for 16 h with either negative control mimics or a 'cocktail' of mimics of miR-208b and miR-499a-5p, along with the HCV PAMP. We then immunoprecipitated Ago2, one of the main miRISC proteins involved in mRNA cleavage, and detected both *IFNL2* and *IFNL3* mRNA among RNA immunoprecipitated together with Ago2 in cells transfected with negative control mimics (**Supplementary Fig. 3f**); this demonstrated recruitment of the miRISC by some endogenous miRNA(s). However, cells treated with the mimics of miR-208b and miR-499a-5p had a significantly greater abundance of *IFNL2* mRNA ($P < 0.01$) and *IFNL3* mRNA ($P < 0.001$) among RNA immunoprecipitated together with Ago2 than did cells transfected with negative control mimics (**Supplementary Fig. 3f**). We also amplified both miR-208b and miR-499a-5p from the Ago2-associated RNA in the cells transfected with mimics of the myomiRs (data not shown). Collectively, these data confirmed that miR-208b and miR-499a-5p directly targeted and destabilized endogenous *IFNL2* and *IFNL3* transcripts.

HCV-induced myomiRs repress *IFNL3*-T transcripts

To investigate the effect of endogenous HCV-induced myomiRs on the *IFNL3* 3′ UTR variants, we developed reporter constructs containing sequence encoding either the red fluorescent protein mCherry or enhanced green fluorescent protein (eGFP) with the

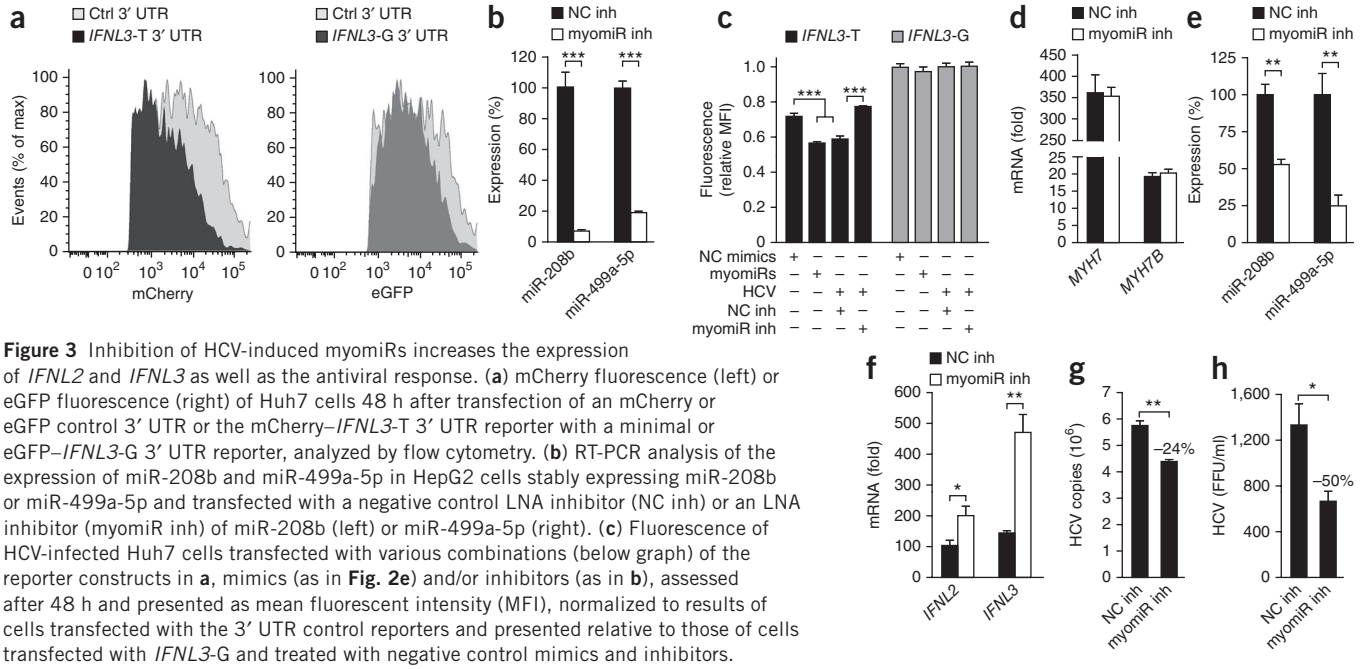

Figure 3 Inhibition of HCV-induced myomiRs increases the expression of *IFNL2* and *IFNL3* as well as the antiviral response. (**a**) mCherry fluorescence (left) or eGFP fluorescence (right) of Huh7 cells 48 h after transfection of an mCherry or eGFP control 3′ UTR or the mCherry–*IFNL3*-T 3′ UTR reporter with a minimal or eGFP–*IFNL3*-G 3′ UTR reporter, analyzed by flow cytometry. (**b**) RT-PCR analysis of the expression of miR-208b and miR-499a-5p in HepG2 cells stably expressing miR-208b or miR-499a-5p and transfected with a negative control LNA inhibitor (NC inh) or an LNA inhibitor (myomiR inh) of miR-208b (left) or miR-499a-5p (right). (**c**) Fluorescence of HCV-infected Huh7 cells transfected with various combinations (below graph) of the reporter constructs in **a**, mimics (as in **Fig. 2e**) and/or inhibitors (as in **b**), assessed after 48 h and presented as mean fluorescent intensity (MFI), normalized to results of cells transfected with the 3′ UTR control reporters and presented relative to those of cells transfected with *IFNL3*-G and treated with negative control mimics and inhibitors. (**d**–**h**) Expression of *MYH7* and *MYH7B* (**d**), miR-208b and miR-499a-5p (**e**) and *IFNL2* and *IFNL3* (**f**), and quantification of HCV viral copy number (**g**) and titer (**h**) in Huh7 cells transfected with inhibitors (as in **b**), then infected with HCV 24 h later and analyzed 72 h after infection, presented relative to results obtained for mock-infected cells (**d**–**f**); numbers above bars (**g**,**h**) indicate percent inhibition relative to that of cells transfected with the negative control LNA inhibitor. FFU, focus-forming units. $*P < 0.05$, $**P < 0.01$ and $***P < 0.001$ (unpaired two-tailed *t*-test). Data are representative of three experiments (**a**) or are from one experiment of three experiments with similar results (**b**–**h**; mean and s.e.m.).

IFNL3-T 3′ UTR or *IFNL3*-G 3′ UTR, respectively, cloned downstream (**Supplementary Fig. 4a**). Those reporter constructs allowed simultaneous expression of the *IFNL3* 3′ UTR variants in the same cells (**Supplementary Fig. 4b**). Flow cytometry of Huh7 cells transfected with those constructs showed a difference in expression of the *IFNL3*-T 3′ UTR and that of the *IFNL3*-G 3′ UTR (**Fig. 3a**), as we had noted before by luciferase assay (**Fig. 1b**). To assess whether the HCV-induced myomiRs repressed the *IFNL3* 3′ UTR variants differently in the same cells, we used that mCherry-eGFP coexpression system along with specific locked nucleic acid (LNA) inhibitors of the induced myomiRs. We designed the LNA inhibitors to inhibit miR-208b and miR-499a-5p with high specificity and demonstrated their efficiency (>75% at 48 h after transfection) in HepG2 cells stably overexpressing miR-208b or miR-499a-5p (**Fig. 3b**). To assess the effect of the inhibitors on HCV-induced myomiRs, we infected Huh7 cells with HCV and then cotransfected them with the mCherry-eGFP *IFNL3* 3′ UTR reporter constructs and LNA inhibitors of myomiRs or control inhibitors. We also compared the mean fluorescent intensity of those cells with that of uninfected cells with the fluorescent reporters in the presence or absence of mimics of myomiRs. Cells infected with HCV suppressed the *IFNL3*-T 3′ UTR reporter but not the *IFNL3*-G 3′ UTR reporter (**Fig. 3c**). The level of repression achieved by the HCV-induced myomiRs was similar to that achieved with the mimics (**Fig. 3c**). Notably, inhibition of miR-208b and miR-499a-5p in infected cells resulted in a significant increase in the expression of *IFNL3*-T but not that of *IFNL3*-G (**Fig. 3c**). Therefore, infection with HCV accelerated the degradation of mRNA bearing the *IFNL3*-T 3′ UTR but not that of mRNA bearing the *IFNL3*-G 3′ UTR, via the induction of myomiRs.

We next assessed the effect of the inhibition of myomiRs on endogenous *IFNL3* transcripts during infection. Huh7 cells infected with HCV are weak producers of interferons because HCV disrupts signaling downstream of the helicase RIG-I, an essential pathogen-recognition receptor of HCV[34–37]. However, *IFNL2* mRNA and *IFNL3* mRNA were detectable in Huh7 cells at 72 h after infection with HCV at a high multiplicity of infection (**Fig. 3d**–**f**), so we used those conditions to study the regulation of *IFNL2* and *IFNL3* mRNA by the myomiRs during infection. Since the genotype of our Huh7 cell line is T/T at the rs4803217 site, we were able to assess the effect of the inhibitors on virus-induced *IFNL3* in the presence of virus-induced myomiRs. Induction of the myosin-encoding genes by HCV was unaffected by the presence of the inhibitors of myomiRs, while the expression of myomiRs was significantly reduced (**Fig. 3d**,**e**). We then measured *IFNL2* and *IFNL3* and found that the inhibitors of myomiRs 'rescued' the expression of *IFNL2* and *IFNL3*, in contrast to the negative control inhibitor (**Fig. 3f**). Furthermore, despite the high multiplicity of infection required for the expression of *IFNL2* and *IFNL3* in this *in vitro* infection system, we observed significantly lower viral copy number and titer in cells treated with the inhibitors of myomiRs than in those treated with negative controls (**Fig. 3g**,**h**). These data demonstrated that HCV-induced miR-208b and miR-499a-5p targeted the rs4803217 SNP in the 3′ UTR of *IFNL3* and that inhibition of myomiRs was able to 'rescue' that suppression.

Induction of myosin and myomiRs during HCV infection

To investigate how HCV induces *MYH7* and *MYH7B*, we infected Huh7.5 cells, which are deficient in innate immunological signaling by RIG-I, and measured myosin expression. Both *MYH7* and *MYH7B*, as well as their respective myomiRs (miR-208b and miR-499a-5p), were induced to levels similar to those observed during infection of Huh7 cells (**Figs. 2c**,**d** and **4a** and **Supplementary Fig. 5a**). We also assessed expression of the myosin-encoding genes in HepG2 cells stimulated with poly(I:C) or the HCV PAMP but did not observe any induction of expression (**Fig. 4b**). Therefore, the induction of *MYH7* and

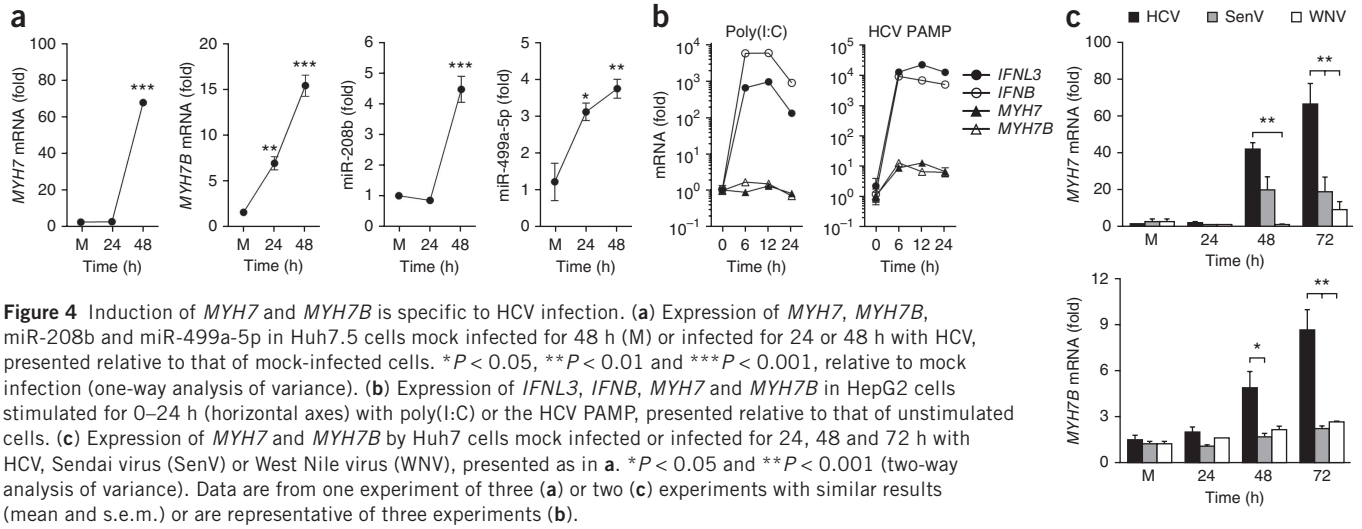

Figure 4 Induction of *MYH7* and *MYH7B* is specific to HCV infection. (**a**) Expression of *MYH7*, *MYH7B*, miR-208b and miR-499a-5p in Huh7.5 cells mock infected for 48 h (M) or infected for 24 or 48 h with HCV, presented relative to that of mock-infected cells. $*P < 0.05$, $**P < 0.01$ and $***P < 0.001$, relative to mock infection (one-way analysis of variance). (**b**) Expression of *IFNL3*, *IFNB*, *MYH7* and *MYH7B* in HepG2 cells stimulated for 0–24 h (horizontal axes) with poly(I:C) or the HCV PAMP, presented relative to that of unstimulated cells. (**c**) Expression of *MYH7* and *MYH7B* by Huh7 cells mock infected or infected for 24, 48 and 72 h with HCV, Sendai virus (SenV) or West Nile virus (WNV), presented as in **a**. $*P < 0.05$ and $**P < 0.001$ (two-way analysis of variance). Data are from one experiment of three (**a**) or two (**c**) experiments with similar results (mean and s.e.m.) or are representative of three experiments (**b**).

MYH7B by HCV occurred independently of HCV PAMP–RIG-I signaling, which indicated that their induction might require viral RNA replication or expression of HCV proteins. To determine whether induction of the myosin-encoding genes was specific to infection with HCV, we also assessed gene expression in Huh7 cells infected with Sendai virus or West Nile virus. Those viruses were unable to induce *MYH7B* and induced only low *MYH7* expression, despite productive infection and induction of *IFNB* (**Fig. 4c** and **Supplementary Fig. 5b**), which indicated that the induction of *MYH7* and *MYH7B* may have been HCV specific.

Myosin and myomiRs in patients with chronic HCV infection

To determine if patients infected with HCV exhibit hepatic expression of the myosin-encoding genes and their associated myomiRs, we evaluated liver RNA recovered from patients chronically infected with HCV. Five of eight patients showed robust expression of *MYH7* that was >200-fold higher than the average expression in uninfected control subjects (**Fig. 5a**). Those patients also had significantly higher expression of *MYH7B* than did the control subjects, albeit at a lower level than *MYH7* (>10-fold higher in five of eight patients; **Fig. 5a**), similar to our observations of *in vitro* HCV infection. Also similar to the results obtained by *in vitro* infection, we did not detect elevated *MYH6* expression (data not shown), which supported the proposal of a specific pathway of induction for *MYH7* and *MYH7B*. Patients infected with HCV also had significantly higher hepatic levels of miR-208b than did uninfected control subjects (**Fig. 5a**). Although those patients had elevated *MYH7B* expression, we did not detect differences between infected patients and uninfected control subjects in mature miR-499a-5p (**Fig. 5a**). To determine whether that observation was caused by an uncoupling of *MYH7B* expression from miR-499a-5p, we also assessed the presence of primary miR-499a transcripts and found significantly elevated levels of those in patients chronically infected with HCV than in uninfected control subjects (**Fig. 5a**). Therefore, our inability to detect mature miR-499a-5p did not seem to be the result of uncoupling from its parental myosin-encoding gene and may have reflected a limitation of the quantitative RT-PCR primers in detecting variations in mature miRNA sequence relative to the reference sequence of mature miR-499a-5p (as in the miRBase microRNA database), which present obstacles for detecting mature miRNA in different tissues[38,39]. However, we did observe a significant correlation between the expression of *MYH7* and that of miR-208b, as well as the expression of *MYH7B* and that of primary miR-499a transcripts, in the patients examined (**Fig. 5b**), which demonstrated that *MYH7* mRNA levels were a reliable 'readout' for miR-208b expression. Overall, these observations demonstrated that HCV induced hepatic expression of genes encoding cardiac and skeletal myosin and their associated myomiRs in HCV-infected patients, in support of the proposed mechanism of repression of *IFNL2* and *IFNL3*-T during infection (**Supplementary Fig. 6**).

DISCUSSION

The work presented here has demonstrated a previously undescribed mechanism by which HCV attenuates the hepatic interferon response. These data suggested that targeted inhibition of miR-208b and miR-499a-5p could 'rescue' the abundance of IFN-λ2 and IFN-λ3 to impart control of HCV infection. Inhibition of miR-122, which is required for HCV replication, has shown promising results in clinical trials demonstrating the feasibility of anti-miRNA therapy[40].

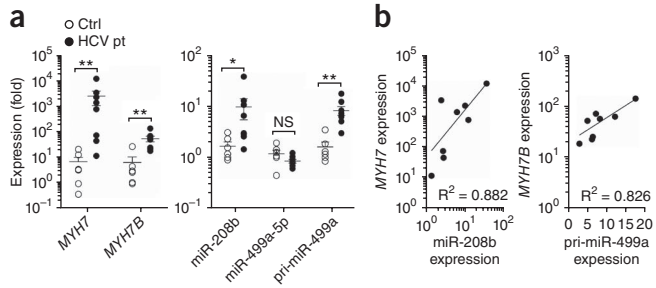

Figure 5 Expression of myosin and myomiRs in patients chronically infected with HCV. (**a**) Expression of *MYH7*, *MYH7B*, miR-208b, miR-499a-5p and primary miR-499a transcripts (pri-miR-499a) among RNA isolated from the livers of patients chronically infected with HCV (HCV pt; $n = 8$) or control subjects (Ctrl; $n = 6$). Each symbol represents an individual subject; small horizontal lines indicate the mean (±s.e.m.). NS, not significant; $*P = 0.02$ and $**P < 0.005$ (two-tailed nonparametric Mann-Whitney test). (**b**) Correlation between *MYH7* expression versus miR-208b expression (Pearson's *r*, $P = 0.0014$) and *MYH7B* expression versus the expression of primary miR-499a transcripts (Pearson's *r*, $P = 0.0033$) in patients infected with HCV; R^2 values (bottom right corners), nonlinear regression. Data are from one experiment.

Therefore, inhibition of HCV-induced myomiRs has the potential to become an important part of treating infection with HCV and mitigating the progression to cirrhosis and liver cancer. As miR-208b and miR-499a-5p are encoded in genes encoding cardiac muscle– and skeletal muscle–specific myosin heavy chains, it is notable that a high prevalence of HCV infection has been reported in patients with hypertrophic cardiomyopathy, dilated cardiomyopathy and myocarditis[41]. Furthermore, autoantibodies to cardiac myosin, including the myosin heavy chains, are commonly observed in patients with those cardiac diseases[42,43], which suggests that aberrant induction of cardiac myosin in the liver by HCV may indirectly contribute to cardiac pathology.

Our comparative analysis of the 3′ UTRs of *IFNL2* and *IFNL3* revealed that despite the significant difference in luciferase expression for the T and G variants of *IFNL3*, the same base-pair change in the 3′ UTR of *IFNL2* did not result in an increase of similar magnitude. If the presence of the G variant in the 3′ UTR of *IFNL3* is the result of genetic selection for increased IFN-λ3 levels during HCV infection, these data may explain why no such variant exists for *IFNL2*; *IFNL2* was expressed at higher levels than the *IFNL3*-T variant, and a T-to-G substitution at position 53 in the 3′ UTR of *IFNL2* resulted in only a small increase in expression. Therefore, such a change in *IFNL2* may not confer a host advantage during infection with HCV. Additionally, IFN-λ3 has been shown to have higher ISG-stimulatory activity than does IFN-λ2, which may make an *IFNL3* escape variant more evolutionarily advantageous, as it has a greater capacity to establish an antiviral state[13,44].

In this study, we have identified a functional *IFNL3* variant associated with clearance of HCV. Our results revealed that the SNP rs4803217 with T-to-G substitution in the 3′ UTR of *IFNL3* resulted in increased expression of *IFNL3* through escape of both AMD and post-transcriptional regulation by HCV-induced miRNAs. By those two mechanisms of post-transcriptional regulation, *IFNL3*-T suffered significantly more degradation than did *IFNL3*-G. A frameshift variant upstream of *IFNL3* has been described that creates the novel gene *IFNL4* (which encodes IFN-λ4)[45]. Expression of *IFNL4* is associated with HCV persistence and a poorer response to therapy with interferon plus ribavirin than that of patients with no *IFNL4* expression[45]. Therefore, it may be the combined effect of *IFNL4* expression and low *IFNL3* expression that makes this haplotype so unfavorable for HCV infection and treatment outcome. However, published work has shown that genes encoding the IFN-λ family are in low linkage disequilibrium in all populations, which suggests that independent positive selection events are targeting these genes[28]. Our data have also shown that HCV infection was specifically able to induce miRNAs that interacted with rs4803217; this may explain why the *IFNL3* locus has been found to be associated only with HCV infection and no other viral infection. Additionally, HCV genotypes may vary in their ability to effectively induce the miRNAs, which may explain why the SNPs of *IFNL3* identified by genome-wide association studies do not uniformly associate with response to therapy across infection with HCV of all genotypes. Thus, the identification of this causal SNP in the 3′ UTR of *IFNL3* provides a potentially important link between host and HCV genetics.

METHODS

Methods and any associated references are available in the online version of the paper.

Note: Any Supplementary Information and Source Data files are available in the online version of the paper.

ACKNOWLEDGMENTS

We thank P. Fink, D. Stetson, E. Clark and C. Lim for critical reading of the manuscript, and S. Badil and M. Hong for technical assistance. Supported by the Department of Immunology of the University of Washington (R.S.), the US National Institutes of Health (AI060389 and AI88778 to M.G., and CA148068 to C.H.H.) and federal funds from the Frederick National Laboratory for Cancer Research of the US National Institutes of Health (HHSN261200800001E) and the Intramural Research Program of the US National Institutes of Health, Frederick National Laboratory for Cancer Research and the National Cancer Institute, Center for Cancer Research (E.B., B.A.S. and M.C.).

AUTHOR CONTRIBUTIONS

A.P.M. and R.S. designed the study and wrote the manuscript; R.S. directed the study; A.P.M. analyzed the data; A.P.M., A.J., R.S. and R.C.J. did ARE and miRNA experiments; S.M.H. did infections and flow cytometry preparations; E.B. and B.A.S. generated base-pairing probabilities; D.A.D. and C.H.H. contributed clinical samples; and M.C. and M.G. provided intellectual input.

COMPETING FINANCIAL INTERESTS

The authors declare no competing financial interests.

1. Ghany, M.G. *et al.* An update on treatment of genotype 1 chronic hepatitis C virus infection: 2011 practice guideline by the American Association for the Study of Liver Diseases. *Hepatology* **54**, 1433–1444 (2011).
2. Pearlman, B.L. Protease inhibitors for the treatment of chronic hepatitis C genotype-1 infection: the new standard of care. *Lancet Infect. Dis.* **12**, 717–728 (2012).
3. Suppiah, V. *et al.* IL28B is associated with response to chronic hepatitis C interferon-α and ribavirin therapy. *Nat. Genet.* **41**, 1100–1104 (2009).
4. Tanaka, Y. *et al.* Genome-wide association of IL28B with response to pegylated interferon-alpha and ribavirin therapy for chronic hepatitis C. *Nat. Genet.* **41**, 1105–1109 (2009).
5. Ge, D. *et al.* Genetic variation in IL28B predicts hepatitis C treatment-induced viral clearance. *Nature* **461**, 399–401 (2009).
6. Rauch, A. *et al.* Genetic variation in IL28B is associated with chronic hepatitis C and treatment failure: a genome-wide association study. *Gastroenterology* **138**, 1338–1345 (2010).
7. Thomas, D.L. *et al.* Genetic variation in IL28B and spontaneous clearance of hepatitis C virus. *Nature* **461**, 798–801 (2009).
8. Kotenko, S.V. *et al.* IFN-λs mediate antiviral protection through a distinct class II cytokine receptor complex. *Nat. Immunol.* **4**, 69–77 (2003).
9. Sheppard, P. *et al.* IL-28, IL-29 and their class II cytokine receptor IL-28R. *Nat. Immunol.* **4**, 63–68 (2003).
10. Witte, K., Witte, E., Sabat, R. & Wolk, K. IL-28A, IL-28B, and IL-29: promising cytokines with type I interferon-like properties. *Cytokine Growth Factor Rev.* **21**, 237–251 (2010).
11. Sommereyns, C., Paul, S., Staeheli, P. & Michiels, T. IFN-lambda (IFN-λ) is expressed in a tissue-dependent fashion and primarily acts on epithelial cells in vivo. *PLoS Pathog.* **4**, e1000017 (2008).
12. Balagopal, A., Thomas, D.L. & Thio, C.L. IL28B and the control of hepatitis C virus infection. *Gastroenterology* **139**, 1865–1876 (2010).
13. Friborg, J. *et al.* Combinations of λ interferon with direct-acting antiviral agents are highly efficient in suppressing hepatitis C virus replication. *Antimicrob. Agents Chemother.* **57**, 1312–1322 (2013).
14. Dickensheets, H., Sheikh, F., Park, O., Gao, B. & Donnelly, R.P. Interferon-lambda (IFN-λ) induces signal transduction and gene expression in human hepatocytes but not in lymphocytes or monocytes. *J. Leukoc. Biol.* **93**, 377–385 (2012).
15. Honda, M. *et al.* Hepatic ISG expression is associated with genetic variation in interleukin 28B and the outcome of IFN therapy for chronic hepatitis C. *Gastroenterology* **139**, 499–509 (2010).
16. McGilvray, I. *et al.* Hepatic cell-type specific gene expression better predicts HCV treatment outcome than IL28B genotype. *Gastroenterology* **142**, 1122–1131 (2012).
17. Naggie, S. *et al.* Dysregulation of innate immunity in hepatitis C virus genotype 1 IL28B-unfavorable genotype patients: impaired viral kinetics and therapeutic response. *Hepatology* **56**, 444–454 (2012).
18. Langhans, B. *et al.* Interferon-λ serum levels in hepatitis C. *J. Hepatol.* **54**, 859–865 (2011).
19. Raglow, Z., Thoma-Perry, C., Gilroy, R. & Wan, Y.J. IL28B genotype and the expression of ISGs in normal liver. *Liver Int.* **33**, 991–998 (2013).
20. Yoshio, S. *et al.* Human blood dendritic cell antigen 3 $(BDCA3)^+$ dendritic cells are a potent producer of interferon-λ in response to hepatitis C virus. *Hepatology* **57**, 1705–1715 (2013).
21. Urban, T.J. *et al.* IL28B genotype is associated with differential expression of intrahepatic interferon-stimulated genes in patients with chronic hepatitis C. *Hepatology* **52**, 1888–1896 (2010).

22. di Iulio, J. *et al.* Estimating the net contribution of interleukin-28B variation to spontaneous hepatitis C virus clearance. *Hepatology* **53**, 1446–1454 (2011).
23. de Castellarnau, M. *et al.* Deciphering the interleukin 28B variants that better predict response to pegylated interferon-α and ribavirin therapy in HCV/HIV-1 coinfected patients. *PLoS ONE* **7**, e31016 (2012).
24. Pedergnana, V. *et al.* Analysis of IL28B variants in an Egyptian population defines the 20 kilobases minimal region involved in spontaneous clearance of hepatitis C virus. *PLoS ONE* **7**, e38578 (2012).
25. Seko, Y., Cole, S., Kasprzak, W., Shapiro, B.A. & Ragheb, J.A. The role of cytokine mRNA stability in the pathogenesis of autoimmune disease. *Autoimmun. Rev.* **5**, 299–305 (2006).
26. Chen, J.M., Ferec, C. & Cooper, D.N. A systematic analysis of disease-associated variants in the 3′ regulatory regions of human protein-coding genes II: the importance of mRNA secondary structure in assessing the functionality of 3′ UTR variants. *Hum. Genet.* **120**, 301–333 (2006).
27. Meisner, N.C. *et al.* mRNA openers and closers: modulating AU-rich element-controlled mRNA stability by a molecular switch in mRNA secondary structure. *Chembiochem.* **5**, 1432–1447 (2004).
28. Manry, J. *et al.* Evolutionary genetic dissection of human interferons. *J. Exp. Med.* **208**, 2747–2759 (2011).
29. Kulkarni, S. *et al.* Differential microRNA regulation of HLA-C expression and its association with HIV control. *Nature* **472**, 495–498 (2011).
30. Guo, H., Ingolia, N.T., Weissman, J.S. & Bartel, D.P. Mammalian microRNAs predominantly act to decrease target mRNA levels. *Nature* **466**, 835–840 (2010).
31. O'Neill, L.A., Sheedy, F.J. & McCoy, C.E. MicroRNAs: the fine-tuners of Toll-like receptor signalling. *Nat. Rev. Immunol.* **11**, 163–175 (2011).
32. van Rooij, E. *et al.* A family of microRNAs encoded by myosin genes governs myosin expression and muscle performance. *Dev. Cell* **17**, 662–673 (2009).
33. Schnell, G., Loo, Y.M., Marcotrigiano, J. & Gale, M. Jr. Uridine composition of the poly-U/UC tract of HCV RNA defines non-self recognition by RIG-I. *PLoS Pathog.* **8**, e1002839 (2012).
34. Foy, E. *et al.* Control of antiviral defenses through hepatitis C virus disruption of retinoic acid-inducible gene-I signaling. *Proc. Natl. Acad. Sci. USA* **102**, 2986–2991 (2005).
35. Li, X.-D., Sun, L., Seth, R.B., Pineda, G. & Chen, Z.J. Hepatitis C virus protease NS3/4A cleaves mitochondrial antiviral signaling protein off the mitochondria to evade innate immunity. *Proc. Natl. Acad. Sci. USA* **102**, 17717–17722 (2005).
36. Sumpter, R. Jr. *et al.* Regulating intracellular antiviral defense and permissiveness to hepatitis C virus RNA replication through a cellular RNA helicase, RIG-I. *J. Virol.* **79**, 2689–2699 (2005).
37. Saito, T. *et al.* Regulation of innate antiviral defenses through a shared repressor domain in RIG-I and LGP2. *Proc. Natl. Acad. Sci. USA* **104**, 582–587 (2007).
38. Chugh, P. & Dittmer, D.P. Potential pitfalls in microRNA profiling. *Wiley Interdiscip. Rev. RNA* **3**, 601–616 (2012).
39. Leshkowitz, D., Horn-Saban, S., Parmet, Y. & Feldmesser, E. Differences in microRNA detection levels are technology and sequence dependent. *RNA* **19**, 527–538 (2013).
40. Janssen, H.L.A. *et al.* Treatment of HCV infection by targeting microRNA. *N. Engl. J. Med.* **368**, 1685–1694 (2013).
41. Matsumori, A. Hepatitis C virus infection and cardiomyopathies. *Circ. Res.* **96**, 144–147 (2005).
42. Lauer, B., Schannwell, M., Kuhl, U., Strauer, B.E. & Schultheiss, H.P. Antimyosin autoantibodies are associated with deterioration of systolic and diastolic left ventricular function in patients with chronic myocarditis. *J. Am. Coll. Cardiol.* **35**, 11–18 (2000).
43. Caforio, A.L. *et al.* Clinical implications of anti-heart autoantibodies in myocarditis and dilated cardiomyopathy. *Autoimmunity* **41**, 35–45 (2008).
44. Dellgren, C., Gad, H.H., Hamming, O.J., Melchjorsen, J. & Hartmann, R. Human interferon-lambda3 is a potent member of the type III interferon family. *Genes Immun.* **10**, 125–131 (2009).
45. Prokunina-Olsson, L. *et al.* A variant upstream of *IFNL3* (*IL28B*) creating a new interferon gene *IFNL4* is associated with impaired clearance of hepatitis C virus. *Nat. Genet.* **45**, 164–171 (2013).

ONLINE METHODS

Cell lines and culture conditions. HepG2, Huh7 or Huh7.5 cells were grown at 37 °C in 5% CO_2 in DMEM (Sigma) medium with 10% heat-inactivated FBS (Atlanta Biologicals) and 1% penicillin-streptomycin-glutamine (Mediatech).

Genotype analysis of rs4803217. The *IFNL3* locus, including the 3′ UTR, was amplified from genomic DNA extracted from HepG2 or Huh7 cells with the following primer pair: forward, 5′-GAGCAGGTGGAATCCTCTTG-3′, and reverse, 5′-AGCAGGCACCTTGAAATGTC-3′. The PCR product was then genotyped at rs4803217 according to the ABI TaqMan genotyping assay procedure with the following primer pair and probes: forward primer, 5′-GCCAGTCATGCAACCTGAGATTTTA-3′, and reverse primer, 5′-AAA TACATAAATAGCGACTGGGTGACA-3′; probe for *IFNL3*-T, 5′-FAM-TTAGCCACTTGTCTTAAT-NFQMGB-3′, and probe for *IFNL3*-G, 5′-VIC-TAGCCACTTGGCTTAAT-NFQMGB-3′ (where 'FAM' is 5-carboxyfluorescein, 'NFQMGB' is a nonfluorescent quencher minor groove binder, and 'VIC' is 6-carboxyrhodamine).

Secondary structure prediction. Per-residue base-pair probabilities of *IFNL3*-T and *IFNL3*-G 3′ UTRs were computed as a column-wise sum of the predicted base probability matrix with the RNAfold program (Vienna RNA package, version 2.0.0, with option '-p')[46].

Construction of human *IFNL2* and *IFNL3* 3′ UTR luciferase reporters. The full-length 3′ UTR (**Supplementary Fig. 1a**) of human *IFNL2* (with T or G at 3′ UTR position 53) or *IFNL3* (with T or G at SNP rs4803217) was cloned into an *Xba*I site downstream of the gene encoding firefly luciferase in the pGL3 reporter vector (Promega). The *IFNL2* and *IFNL3*-T 3′ UTR luciferase constructs with disrupted AREs were created by the introduction of C instead of T (ATTTA→ATCTA) in all three ATTTA motifs (synthesized by Life Technologies). *IFNL3*-T 3′ UTRs with individual ARE sites disrupted were synthesized and subcloned into the pGL3 vector. The following primers were used to introduce, by site-directed mutagenesis (Stratagene), a T-to-G substitution at position 53 in *IFNL3*-G(ΔARE) and individual mutant ARE constructs: forward 5′-TTTATCTATAAATTAGCCACTTGTCTTAATCTAT TGTCACCCAGTCG-3′ and reverse 5′-CGACTGGGTGACAATAGATTAAG ACAAGTGGCTAATTTATAGATAAA-3′.

miRNA-target pairing-site prediction. Bioinformatics analysis with the RNAhybrid tool for finding the minimum free energy hybridization (RNAhybrid version 2.2)revealed a potential miRNA-binding site for miR-208b and miR-499a-5p at rs4803217 in the *IFNL3*-T 3′ UTR and *IFNL2* 3′ UTR. Positions 43–59 in the *IFNL3*-T 3′ UTR were predicted to pair with those myomiRs.

Cell transfection and reporter assays. For luciferase assays, HepG2 or Huh7 cells were plated at a density of 1×10^4 cells per well in a 96-well plate and grown overnight. Cells were transfected with 20–40 ng per well of pGL3 and 0.1–0.5 ng per well of renilla luciferase reporter constructs with X-tremeGENE 9 DNA transfection reagent (0.2 µl per well; Roche). Cotransfection experiments with 20 nM of mimics of miR-208b and miR-499a-5p (Dharmacon) were conducted with DharmaFECT Duo transfection reagent (0.1–0.2 µl per well; Dharmacon). A negative control mimic that does not bind to any target in mammalian genes (Dharmacon) was included in all experiments as needed. After 48 h of incubation, cells were lysed and the firefly and renilla luciferase activity was measured with the Dual-Luciferase Reporter Assay System (Promega) and a multi-mode microplate reader (Synergy HT; BioTek). Luciferase activity is presented as percent of the ratio of firefly luciferase activity to renilla luciferase activity. For coexpression experiments with mCherry and eGFP reporter constructs, Huh7 cells (uninfected or infected with HCV) in a 48-well plate were transfected DharmaFECT Duo transfection reagent (1 µl per well) with 50 ng of total plasmid (controls and *IFNL3* 3′ UTR reporters mixed at a ratio of 1:1) along with 40 nM of a 'cocktail' of LNA inhibitors of miR-208b and miR-499a-5p (designed with Exiqon). The negative control inhibitor was LNA mismatched to miR-208b and miR-499a-5p. For studies of the endogenous regulation of *IFNL2* and *IFNL3* mRNA by HCV-induced myomiRs, Huh7 cells were plated at a density of 3×10^5 cells per well in 2 ml of a six-well plate and, 8 h later, were transfected with 40 nM of inhibitors (of myomiRs or negative control inhibitors). At 16 h after transfection, cells were washed and replated into 12-well dishes at a density of 1×10^5 cells per well and were infected with HCV after 6 h.

For analysis of the effect of miR-208b and miR-499a-5p on endogenous expression of *IFNL2* and *IFNL3*, HepG2 cells were plated at a density of 3×10^5 cells per well in a six-well plate in 2 ml and were grown overnight. The mimics of miR-208b and miR-499a-5p (20 nM) were transfected into cells with the DharmaFECT 4 transfection reagent (5 µl per well). After 24 h of incubation, cells were transfected and/or stimulated with poly(I:C) (3 µg per well; InvivoGen) with X-tremeGENE 9 transfection reagent (3 µl per well) according to the manufacturer's instructions (Roche). For experiments involving the HCV PAMP (the 3′ poly-U/UC tract)[33,47], the mimics of miR-208b and miR-499a-5p (20 nM) plus 100 or 500 ng of the PAMP were transfected into HepG2 cells with the DharmaFECT Duo transfection reagent (3 µl per well).

Cell lines overexpressing pLV-miRNA. Lentiviral vectors producing miR-208b or miR-499a-5p were transduced into HepG2 cells by lentiviral infection as described[48]. Self-inactivating pLV-miR-208b, pLV-miR-499a-5p or pLV-control constructs (Biosettia) were used to generate vesicular stomatitis virus–pseudotyped lentiviral vectors. The pLV constructs were transfected into HEK293FT cells with FuGENE 6 according to the manufacturer's instructions (Roche). HepG2 cells were transduced by lentivirus. After transduction, the cells were selected with 5 µg/ml puromycin (Sigma-Aldrich). The expression of miRNA was evaluated by real-time PCR probing for mature miR-208b and miR-499-5p.

RNA and miRNA expression analysis by RT-PCR. RNA was extracted with the RNeasy Kit (Qiagen) and reverse-transcribed with a QuantiTect RT kit (Qiagen). RT-PCR primers and probes previously designed and tested for specificity were used for the detection of *IFNL2* and *IFNL3* as follows[21]: 900 nM *IFNL2* forward (5′-GAAGGTTCTGGAGGCCACC-3′) and 900 nM *IFNL2* reverse (5′-GGCTGGTCCAAGACGTCCA-3′); 900 nM *IFNL3* forward 5′-GAAGGTTCTGGAGGCCACC-3′ and 900 nM *IFNL3* reverse 5′-GGCTGGTCCAAGACATCC-3′; 250 nM probe 5′-FAM-GCTGACACTGACCCAGCCCTGG-TAMRA-3′. TaqMan RT-PCR assays (Life Technologies) were used for quantification of human *IFNB1*, *MYH6*, *MYH7*, *MYH7B* and primary miR-499a transcripts. *HPRT* and *GAPDH* (Integrated DNA Technologies) served as endogenous controls.

miRNA was extracted with TRIzol (Invitrogen). Mature hsa-miR-208b and hsa-miR-499a-5p were quantified by miRCURY LNA Universal RT microRNA PCR assays according to the manufacturer's instructions (Exiqon). Among the commercially available miRNA primers, we found the Exiqon LNA primers for miR-208b and miR-499a-5p had superior efficiency. Three Exiqon LNA primers designed to detect the most common variations in mature miRNA sequence relative to the reference sequence of mature miR-499a-5p (in the miRBase microRNA database) were pooled for detection. The miR-208b Exiqon LNA primer was optimized through the use of primers with a lower melting temperature. SNORD38B was used as an endogenous control. The stability of mRNA was assessed with 10 µg actinomycin D per 1×10^6 cells per ml. For analysis of the stability of firefly luciferase mRNA, total RNA was extracted (Qiagen) and poly(A) mRNA was purified from the preparation with a Dynabead mRNA Purification Kit (Ambion/Life Technologies). Firefly luciferase mRNA was detected with custom-designed TaqMan primers (Life Technologies). Samples containing no reverse transcripase were included and showed no amplification.

Flow cytometry. Huh7 cells were assessed by flow cytometry with an LSR II (BD Biosciences). For all experiments, cells were fixed for 30 min in 3% paraformaldehyde in 1× PBS.

Coimmunoprecipitation of mRNA and miRNA from the miRISC. mRNA-miRNA-protein complexes were immunoprecipitated as described[49]. 3×10^6 HepG2 cells were plated in 10-cm^2 dishes and grown overnight. Each plate was transfected with 20 nM of the negative control mimic or a 'cocktail' of miR-208b and miR-499a-5p, as well as 2 µg HCV PAMP with 5 µl

doi:10.1038/ni.2758

DharmaFECT Duo transfection reagent. At 16 h after transfection, cells were lysed in polysome lysis buffer. An aliquot of the lysate was used to obtain the input *HPRT* mRNA values for normalization. Lysates were precleared for 1 h with protein G beads (17-0618-02; GE Healthcare) followed by overnight immunoprecipitation with 10 μg of control immunoglobulin G (MAB002; R&D Systems) or antibody to Ago2 (015-22031; Wako) conjugated to protein G beads. Immunoprecipitates were washed with polysome lysis buffers and aliquots were used for immunoblot analysis of Ago2 (015-22031; Wako) and for detection of RNA for *IFNL2*, *IFNL3*, miR-208b and miR-499a-5p.

Viral infection of Huh7 and Huh7.5 cell lines. The cell culture–adapted HCV JFH1 genotype 2A strain was propagated, and infectivity titrated by focus-forming assay as described[50]. For HCV-infection experiments, cells were inoculated for 3 h with virus (multiplicity of infection, 0.3 or 10) and then the medium was replaced. Cells were harvested with TRIzol at the appropriate times. The copy number of HCV RNA was measured by quantitative real-time PCR with a TaqMan Fast Virus 1-step kit and primers specific for the 5′ UTR (Pa03453408_s1, Life Technologies). The copy number was calculated by comparison to a standard curve of *in vitro*–transcribed full-length HCV RNA. Sendai virus strain Cantell was from Charles River Laboratory. Stocks of West Nile virus (TX strain[51]) were generated by a single round of amplification on Vero-E6 African green monkey epithelial cells (ccl-81; American Type Culture Collection) and supernatants were collected, divided into aliquots and stored at −80 °C. Viral stocks were titered by standard plaque assay on BHK21 baby hamster kidney cells as described[52].

Liver biospecimens. Liver tissue of patients chronically infected with HCV or from uninfected control subjects was obtained with the approval of the University of Utah Institutional Review Board, and the participants provided written informed consent approved by the University of Utah ethics committee. Unused samples from percutaneous biopsies of patients chronically infected with HCV (n = 8) with no pathological evidence of fibrosis (mild HCV; Metavir grade 1, stage 0) were analyzed. Control liver tissue was obtained from unused donor liver (n = 6) with approval of the Institutional Review Board. All liver samples were 'flash frozen' in liquid nitrogen after collection and were stored at −80 °C.

46. Lorenz, R. *et al.* ViennaRNA package 2.0. *Algorithms Mol. Biol.* **6**, 26 (2011).
47. Saito, T., Owen, D.M., Jiang, F., Marcotrigiano, J. & Gale, M. Jr. Innate immunity induced by composition-dependent RIG-I recognition of hepatitis C virus RNA. *Nature* **454**, 523–527 (2008).
48. Savan, R., Chan, T. & Young, H.A. Lentiviral gene transduction in human and mouse NK cell lines. *Methods Mol. Biol.* **612**, 209–221 (2010).
49. Peritz, T. *et al.* Immunoprecipitation of mRNA-protein complexes. *Nat. Protoc.* **1**, 577–580 (2006).
50. Kato, T. *et al.* Cell culture and infection system for hepatitis C virus. *Nat. Protoc.* **1**, 2334–2339 (2006).
51. Keller, B.C. *et al.* Resistance to α/β interferon is a determinant of West Nile virus replication fitness and virulence. *J. Virol.* **80**, 9424–9434 (2006).
52. Diamond, M.S., Shrestha, B., Marri, A., Mahan, D. & Engle, M. B cells and antibody play critical roles in the immediate defense of disseminated infection by West Nile encephalitis virus. *J. Virol.* **77**, 2578–2586 (2003).